Simultaneously Modeling the Convection Zone and Corona at Large Spatial Scales

W.P. Abbett

and

G.H. Fisher, B.T. Welsch, D.J. Bercik

Space Sciences Laboratory, Univ. of California, Berkeley

Solar cycle 24: Dec 2008, Napa, CA

Motivation:

Understanding the physics of the solar magnetic field ---

- from its ***generation*** in the turbulent, differentially-rotating interior
- to the ultimate ***release of magnetic energy*** in the atmosphere in the form of radiation, solar wind acceleration, flares or CMEs ---

requires

- an understanding of the dynamic, energetic and magnetic connection between the convective interior and corona.

Our Principal Challenge:

To describe the complex interaction between the solar envelope and atmosphere in the simplest way possible that still allows for a quantitative study of the solar magnetic field over the spatial and temporal scales characteristic of active regions.

Characteristics of the convective interior:

- The convection zone is high-density, high-β, optically-thick, turbulent plasma.
- Magnetic fields entrained within convective flows at and below the visible surface evolve slowly compared to the coronal field.

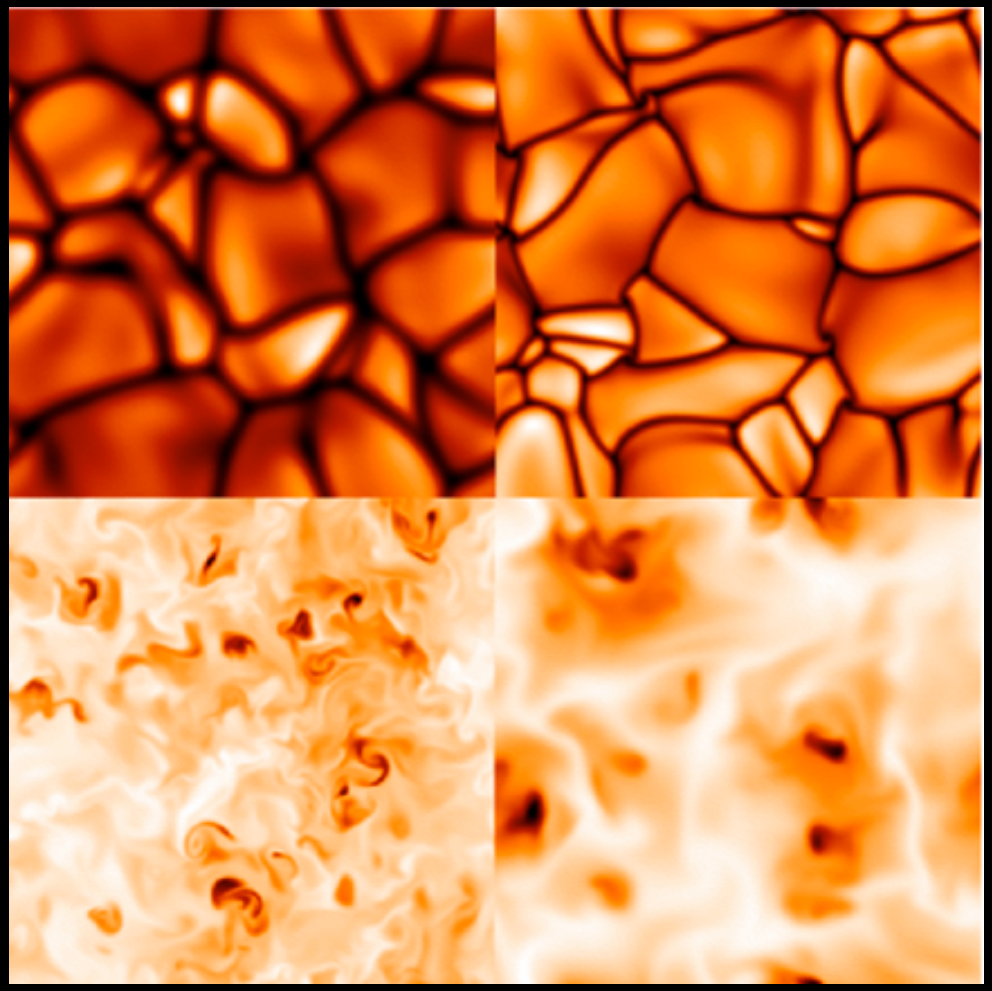

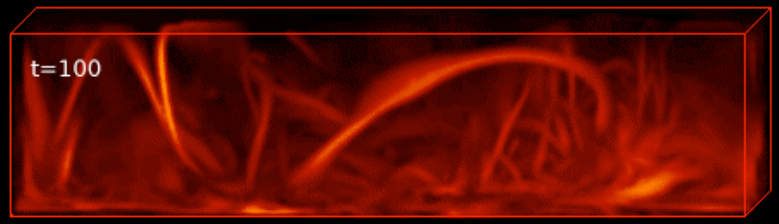

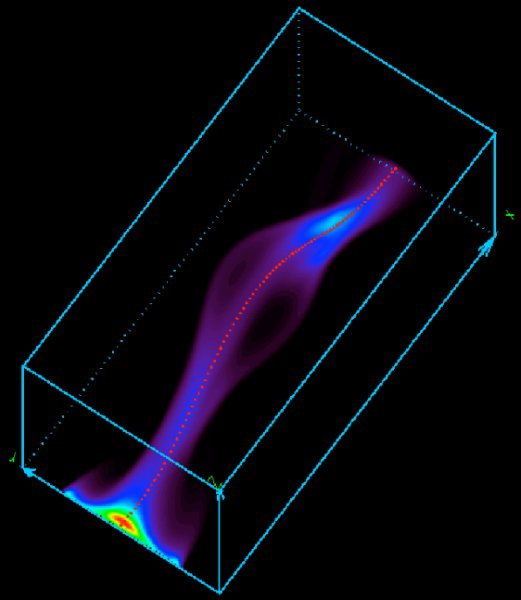

MHD models of the deep interior (from Abbett et al. 2000, 2004)

Characteristics of the solar corona:

- The corona is a low-density, low-β, optically-thin, hot plasma
- Plasma within coronal loops evolves rapidly compared to sub-surface structures
- The corona can store energy over long periods of time, but can then undergo sudden, rapid, and dramatic changes as magnetic energy is released.

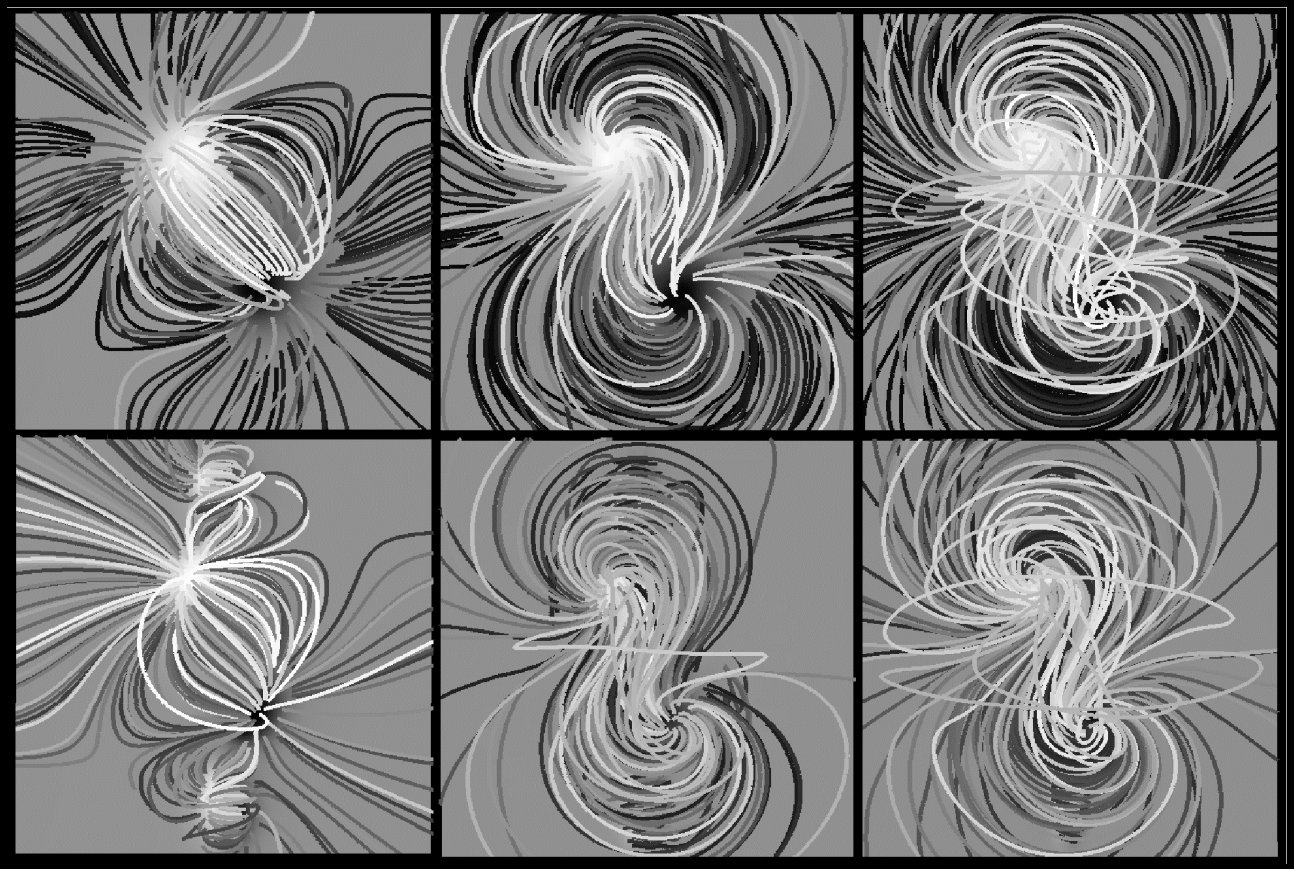

A comparison of potential field (left column), and non-linear force-free field extrapolations (middle column) to a Magara (2004) ideal MHD simulation of active region-scale flux emergence without convective turbulence (right column). The fieldlines of the top (bottom) row are generated from a synthetic magnetogram positioned in the model chromosphere (photosphere). Image from Abbett et. al. (2004).

Modeling the combined convection zone-to-corona system in an efficient, yet physically self-consistent way:

The resistive fully-compressible MHD system of equations:

$$\frac{\partial \rho}{\partial t} + \nabla \cdot (\rho \mathbf{u}) = 0$$

$$\frac{\partial \rho \mathbf{u}}{\partial t} + \nabla \cdot \left[\rho \mathbf{u}\mathbf{u} + \left(p + \frac{B^2}{8\pi} \right) \mathbf{I} - \frac{\mathbf{B}\mathbf{B}}{4\pi} - \mathbf{D} \right] = \rho \mathbf{g}$$

$$\frac{\partial B}{\partial t} + \nabla \cdot (\mathbf{u}\mathbf{B} - \mathbf{B}\mathbf{u}) = -\nabla \times \eta (\nabla \times \mathbf{B})$$

$$\frac{\partial e}{\partial t} + \nabla \cdot (e\mathbf{u}) = -p \nabla \cdot \mathbf{u} + \frac{\eta}{4\pi} \left| \nabla \times \mathbf{B} \right|^2 + \phi + Q$$

Closure relation: a non-ideal equation of state obtained through an inversion of the OPAL tables (Rogers 2000),

$$p = p(\rho, e)$$

The source term Q in the energy equation,

$$\frac{\partial e}{\partial t} + \nabla \cdot (e\mathbf{u}) = -p\nabla \cdot \mathbf{u} + \frac{\eta}{4\pi}\left|\nabla \times \mathbf{B}\right|^2 + \phi + Q$$

must include the important physics believed to govern the evolution of the combined system.

In the corona, this includes

- radiative cooling in the optically thin limit,
- the divergence of the electron heat flux,
- a coronal heating mechanism.

In the lower atmosphere at and above the visible surface,

- radiative cooling (optically thick)

Below the surface in the deeper layers of the convective interior

- radiative cooling (in the optically thick diffusion limit)

We represent the source term Q as follows:

$$Q = Q_r + Q_c + Q_B$$

In order to extend the spatial domain to active region scales, we choose not to solve the optically-thick LTE transfer equation to obtain an expression for surface cooling, Q_r. **Instead, we choose to approximate this cooling in a way that successfully reproduces the average stratification and solar-like convective turbulence of the more realistic simulations of Bercik (2002) and Stein et al. (2003)**:

$$Q_r = \xi_1 Q_1 + \xi_2 Q_2 + \xi_3 Q_3 \qquad \text{where} \qquad \begin{aligned} Q_1 &= -n_e n_h \Lambda(T) \\ Q_2 &= \tau^{-1}\left[e - e(\rho, T_0)\right] \\ Q_3 &= \nabla \cdot \left[\kappa_R(\rho, T)\nabla T\right] \end{aligned}$$

and ξ_1, ξ_2, and ξ_3 represent dimension-less envelope functions that restrict each term to the appropriate range of densities in such a way as to avoid sharp cutoffs. $\Lambda(T)$ is obtained from the CHIANTI atomic database.

The structure of the transition region and corona depend strongly on the remaining non-radiative terms in $Q = Q_r + Q_c + Q_B$: the divergence of the electron heat flux,

$$Q_c = \xi \, \mathbf{B} \cdot \nabla \left(\kappa_{\|}(T) \, \mathbf{B} \cdot \frac{\nabla T}{B^2} \right)$$

and an additional coronal heating rate, Q_B . We employ an empirically-based description of coronal heating consistent with the observed relationship between unsigned magnetic flux and the power dissipated in the atmosphere by a coronal heating mechanism, $\int Q_B dV = c\Phi^{\alpha}$.

The RHS of this equation represents the Pevtsov et al. (2003) power law relationship between X-ray luminosity and unsigned magnetic flux at the photosphere $L_x = c\Phi^{\alpha}$. If we choose a simple heating function of the form $Q_B \propto B / \langle B \rangle$ (consistent with Lundquist et al. 2008), we arrive at the empirically-based form of coronal heating used in the quiet Sun models of Abbett (2007):

$$Q_B = \frac{c\Phi^{\alpha} B}{\int B dV}$$

The calibrated radiative source term Q_r in $Q = Q_r + Q_c + Q_B$, coupled with a constant radiative flux lower boundary condition (on average) maintains the super-adiabatic stratification necessary to initiate and sustain convection.

The thermodynamic structure of the model is controlled by the energy source terms, the gravitational acceleration and the applied thermodynamic boundary conditions. No stratification is imposed a priori.

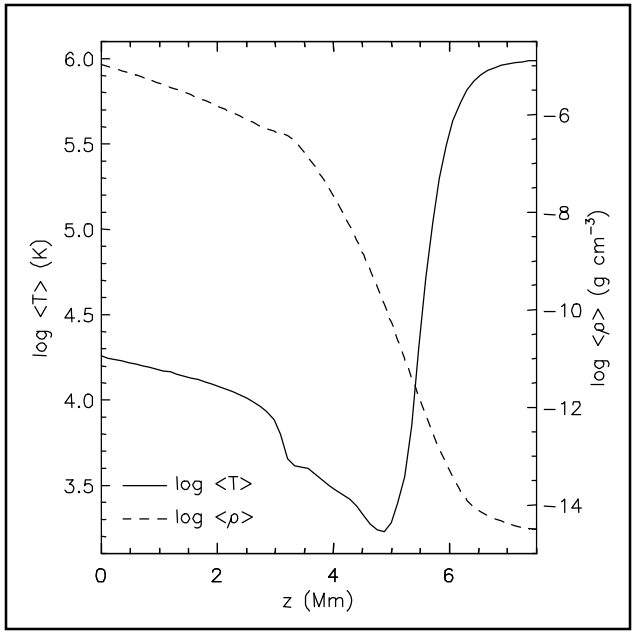

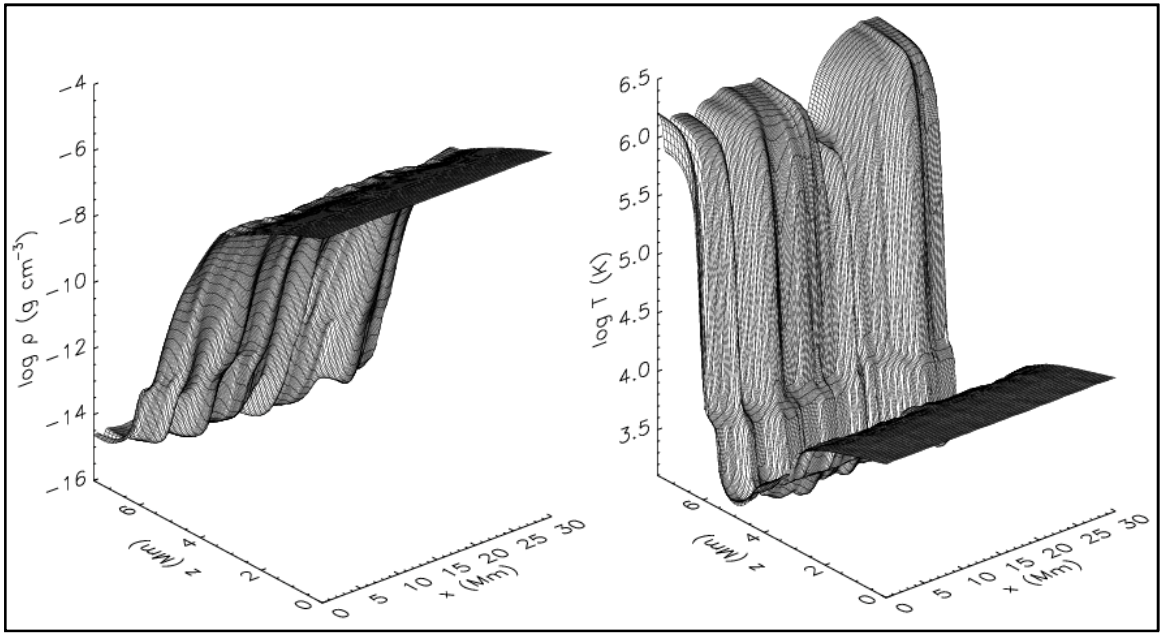

Numerical challenges:

A dynamic numerical model extending from below the photosphere out into the corona must:

- span a ~ 10 - 15 order of magnitude change in gas density and a thermodynamic transition from the 1 MK corona to the optically thick, cooler layers of the low atmosphere, visible surface, and below;

- resolve a ~ 100 km photospheric pressure scale height while simultaneously following large-scale evolution (we use the Mikic et al. 2005 technique to mitigate the need to resolve the 1 km transition region scale height characteristic of a Spitzer-type conductivity);

- remain highly accurate in the turbulent sub-surface layers, while still employing an effective shock capture scheme to follow and resolve shock fronts in the upper atmosphere

- address the extreme temporal disparity of the combined system

RADMHD: Numerical techniques

- We use a semi-implicit, operator-split method.

$$\frac{\partial \rho}{\partial t} + \nabla \cdot (\rho \mathbf{u}) = 0$$

$$\frac{\partial \rho \mathbf{u}}{\partial t} + \nabla \cdot \left[\rho \mathbf{u}\mathbf{u} + \left(p + \frac{B^2}{8\pi} \right) \mathbf{I} - \frac{\mathbf{B}\mathbf{B}}{4\pi} - \mathbf{D} \right] = \rho \mathbf{g}$$

$$\frac{\partial B}{\partial t} + \nabla \cdot (\mathbf{u}\mathbf{B} - \mathbf{B}\mathbf{u}) = -\nabla \times \eta (\nabla \times \mathbf{B})$$

$$\frac{\partial e}{\partial t} + \nabla \cdot (e\mathbf{u}) = -p \nabla \cdot \mathbf{u} + \frac{\eta}{4\pi} |\nabla \times \mathbf{B}|^2 + \phi + Q$$

- **Explicit sub-step:** We use a 3D extension of the **semi-discrete** method of Kurganov & Levy (2000) with the third order-accurate central weighted essentially non-oscillatory **(CWENO)** polynomial reconstruction of Levy et al. (2000).

- **CWENO interpolation** provides an efficient, accurate, simple shock capture scheme that allows us to resolve shocks in the transition region and corona without refining the mesh. The solenoidal constraint on **B** is enforced implicitly.

- We use a semi-implicit, operator-split method

$$\frac{\partial \rho}{\partial t} + \nabla \cdot (\rho \mathbf{u}) = 0$$

$$\boxed{\frac{\partial \rho \mathbf{u}}{\partial t}} + \nabla \cdot \left[\rho \mathbf{u}\mathbf{u} + \left(p + \frac{B^2}{8\pi} \right) \mathbf{I} - \frac{\mathbf{B}\mathbf{B}}{4\pi} - \boxed{\mathbf{D}} \right] = \rho \mathbf{g}$$

$$\boxed{\frac{\partial B}{\partial t}} + \nabla \cdot (\mathbf{u}\mathbf{B} - \mathbf{B}\mathbf{u}) = \boxed{-\nabla \times \eta (\nabla \times \mathbf{B})}$$

$$\boxed{\frac{\partial e}{\partial t}} + \nabla \cdot (e\mathbf{u}) = -p \nabla \cdot \mathbf{u} + \boxed{\frac{\eta}{4\pi} |\nabla \times \mathbf{B}|^2 + \phi + Q}$$

- **Implicit sub-step:** We use a **"Jacobian-free" Newton-Krylov (JFNK)** solver (see Knoll & Keyes 2003). The Krylov sub-step employs the generalized minimum residual **(GMRES)** technique.

- **JFNK** provides a memory-efficient means of implicitly solving a non-linear system, and frees us from the restrictive CFL stability conditions imposed by e.g., the electron thermal conductivity and radiative cooling.

- The MHD system is solved on a domain-decomposed mesh.

- Spatial disparities of the combined convection zone-to-corona system are addressed via the CWENO explicit scheme, the domain decomposition strategy, and a non-uniform mesh as necessary.

- Temporal disparities of the combined convection zone-to-corona system are addressed via the JFNK implicit scheme. Pre-conditioning or adjustable error criteria are essential requirements if one wishes to rapidly relax atmospheres by significantly exceeding the CFL limit.

- Boundary conditions applied to the convective relaxation runs: Periodic in the transverse directions, constant radiative flux in through a closed lower boundary, and an open coronal boundary

Recent Improvements and enhancements to RADMHD:

To extend the quiet Sun simulations to active region spatial scales, certain enhancements and improvements to the numerical algorithms were necessary. We describe some of these in more detail below:

- The code has been successfully ported to NASA's supercomputing cluster "Discover", and the spatial scale of the Abbett (2007) quiet Sun simulations has been significantly extended. The current runs use 128 processors on Discover and with a spatial extent of ~ 75 x 38 x 14 Mm^3 and resolution of ~ 100 km^3.

- The table inversion and interpolation procedures for incorporating the non-ideal equation of state (using the OPAL package), and optically thin cooling (using the CHIANTI atomic database) have been updated to significantly improve performance and load balancing characteristics on large scale, multi-processor platforms.

- The parameterized energy source term mimicking optically thick surface cooling has been simplified so as to more easily transition to the physics-based optically thin treatment as densities decrease in the upper chromosphere. The number of adjustable parameters in the envelope functions has been cut in half.

- In anticipation of greater temporal disparities in the active region runs, we have been developing "adaptive convergence criteria" within the implicit JFNK solver. These schemes dynamically adapt the error metric, used to determine whether or not to accept the next guess, to the accuracy of the last guess: If the last guess was wildly inaccurate, the error criterion is loosened, allowing the JFNK sub-step to take the next guess with relatively few iterations. If the last guess has improved, the error criterion is tightened to ensure the next guess is yet more accurate. We have found empirically that using such schemes greatly reduce the total number of iterations required to converge to the final JFNK solution at a given time step, particularly when the initial guess (e.g., the solution for the state vector at the previous time step) is poor.

In addition, the publicly available alpha test version of RADMHD was optimized, and reorganized to maximize portability. The development team* has been testing RADMHD on a number of different Fortran compilers (including Intel, Absoft, Lahey, gfortran, and NAG), and on a number of distinctly different platforms (ranging from the ASUS Eee PC to NASA's Discover supercomputer).

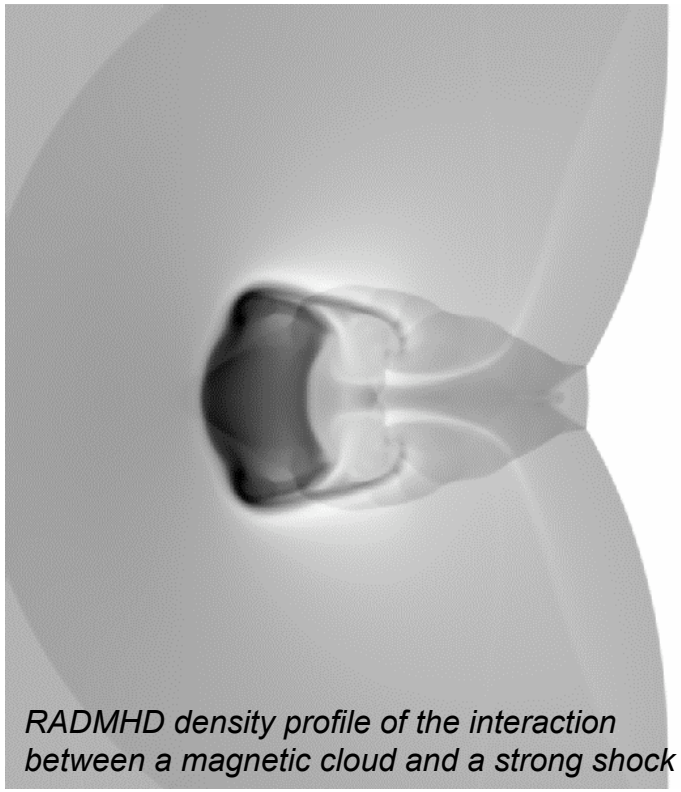

RADMHD density profile of the interaction between a magnetic cloud and a strong shock

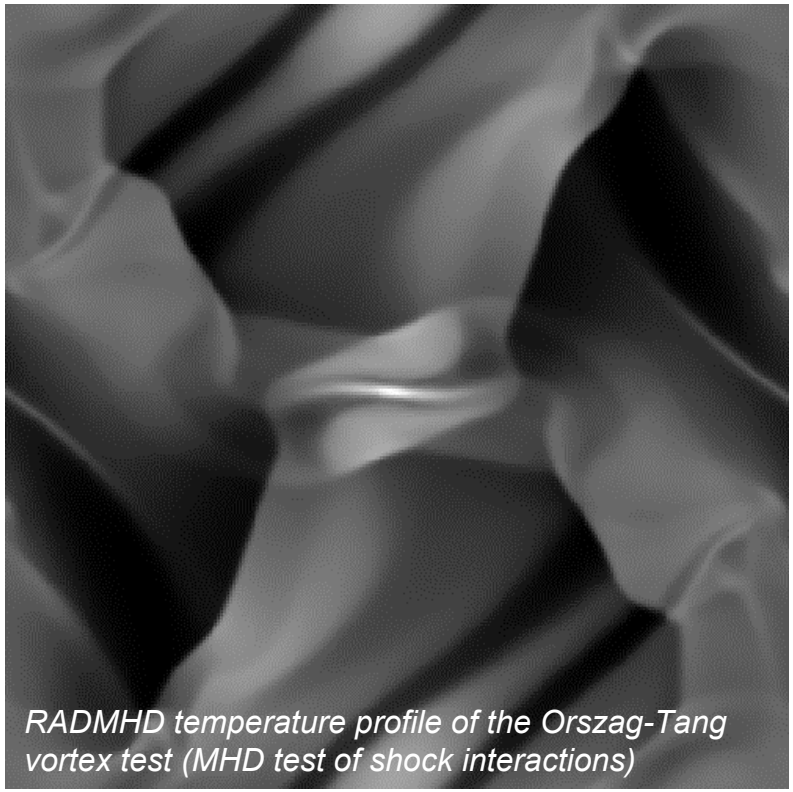

RADMHD temperature profile of the Orszag-Tang vortex test (MHD test of shock interactions)

* Abbett, Bercik, Fang, Fisher, Huba, Manchester, McTiernan, Roussev, Schuck, Welsch (SSL Berkeley, NRL, Univ. of Hawaii, Univ. of Michigan)

The quiet Sun magnetic field in the model chromosphere

Magnetic field generated through the action of a convective surface dynamo.

Fieldlines drawn (in both directions) from points located 700 km above the visible surface.

Grayscale image represents the vertical component of the velocity field at the model photosphere.

The low-chromosphere acts as a dynamic, high-β plasma except along thin rope-like structures threading the atmosphere, connecting strong photospheric structures to the transition region-corona interface.

Plasma-β ~ 1 at the photosphere only in localized regions of concentrated field (near strong high-vorticity downdrafts

From Abbett (2007)

Flux submergence in the quiet Sun and the connectivity between an initially vertical coronal field and the turbulent convection zone

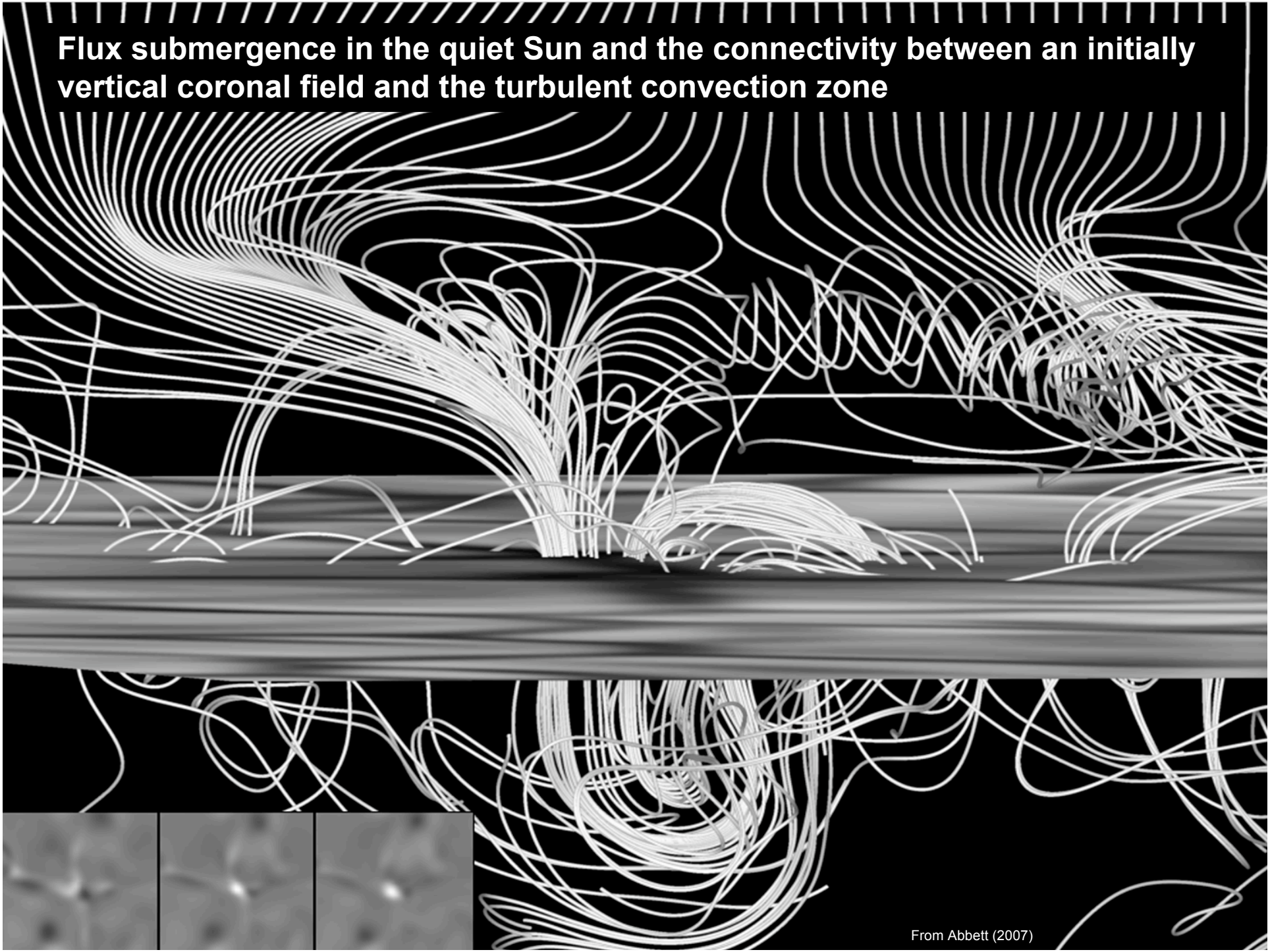

From Abbett (2007)

Recent results: a pre-emergence model photosphere

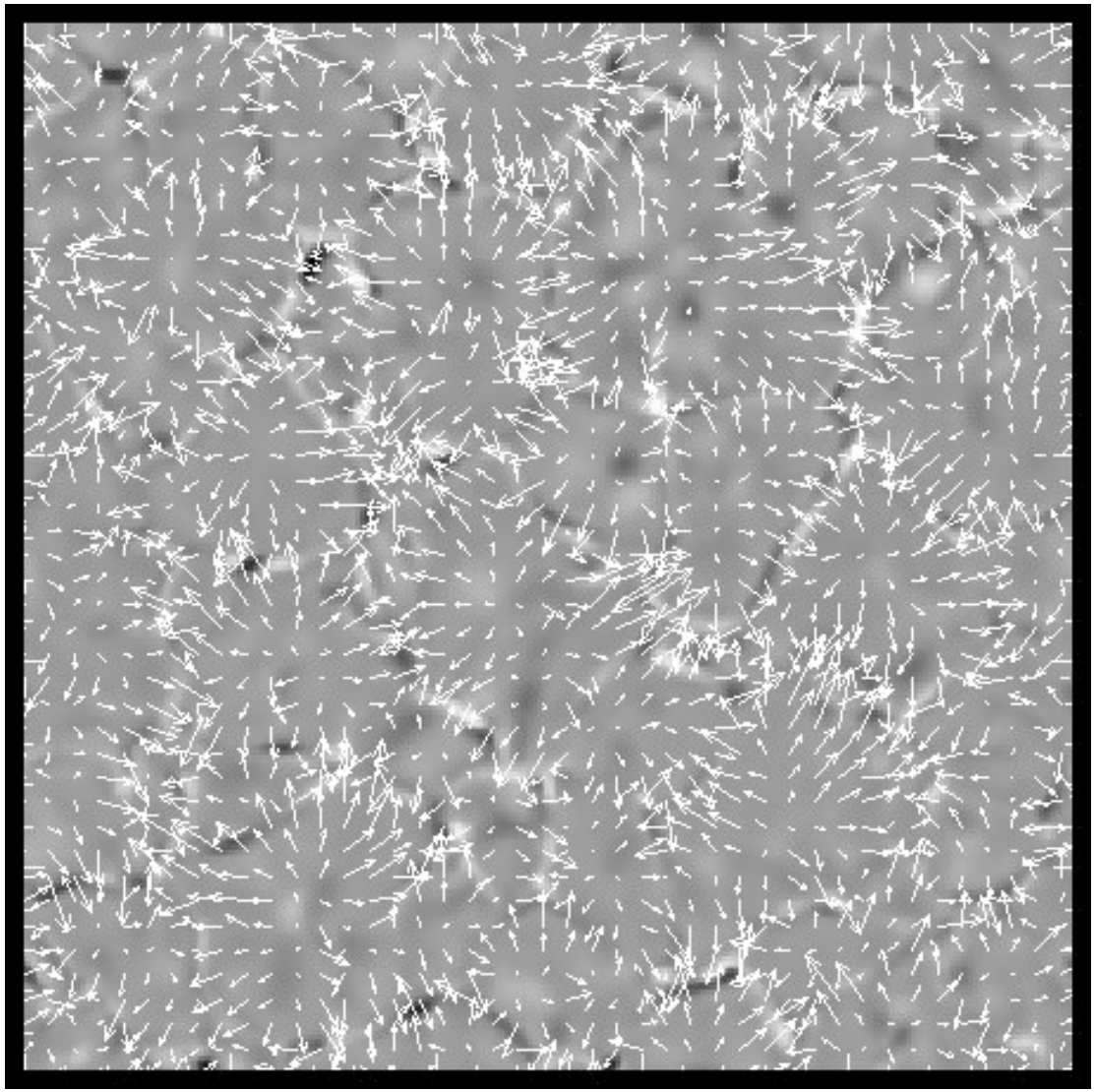

Vertical component of the magnetic field (grayscale) and the transverse flow pattern (vectors) in the model photosphere.

Given the importance of flows in determining electric fields, and the transport of magnetic energy and helicity into the corona, we take a convective relaxation simulation and ask the question:

How well do flows observed at the surface correspond to flows higher in the atmosphere?

Are photospheric electric fields appropriate drivers for coronal models whose boundary lies high in the chromosphere near the transition region boundary?

The corresponding model chromosphere

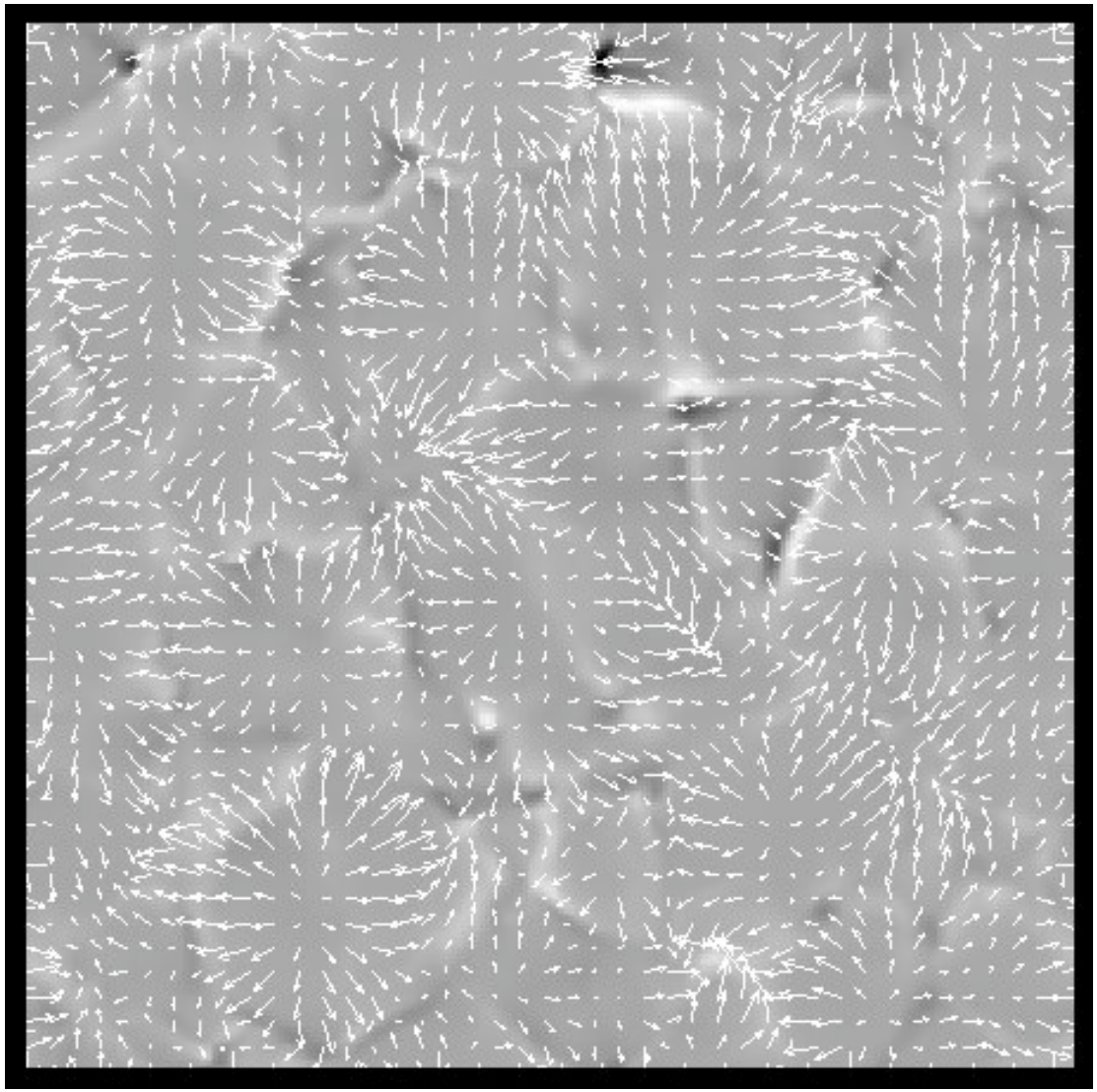

Vertical component of the magnetic field (grayscale) and the transverse flow pattern (vectors) in the model chromosphere.

A horizontal slice taken ~ 400 km above the model photosphere. Note that there are significant differences between the chromospheric and photospheric flow patterns in and around concentrations of magnetic flux.

The corresponding model transition region

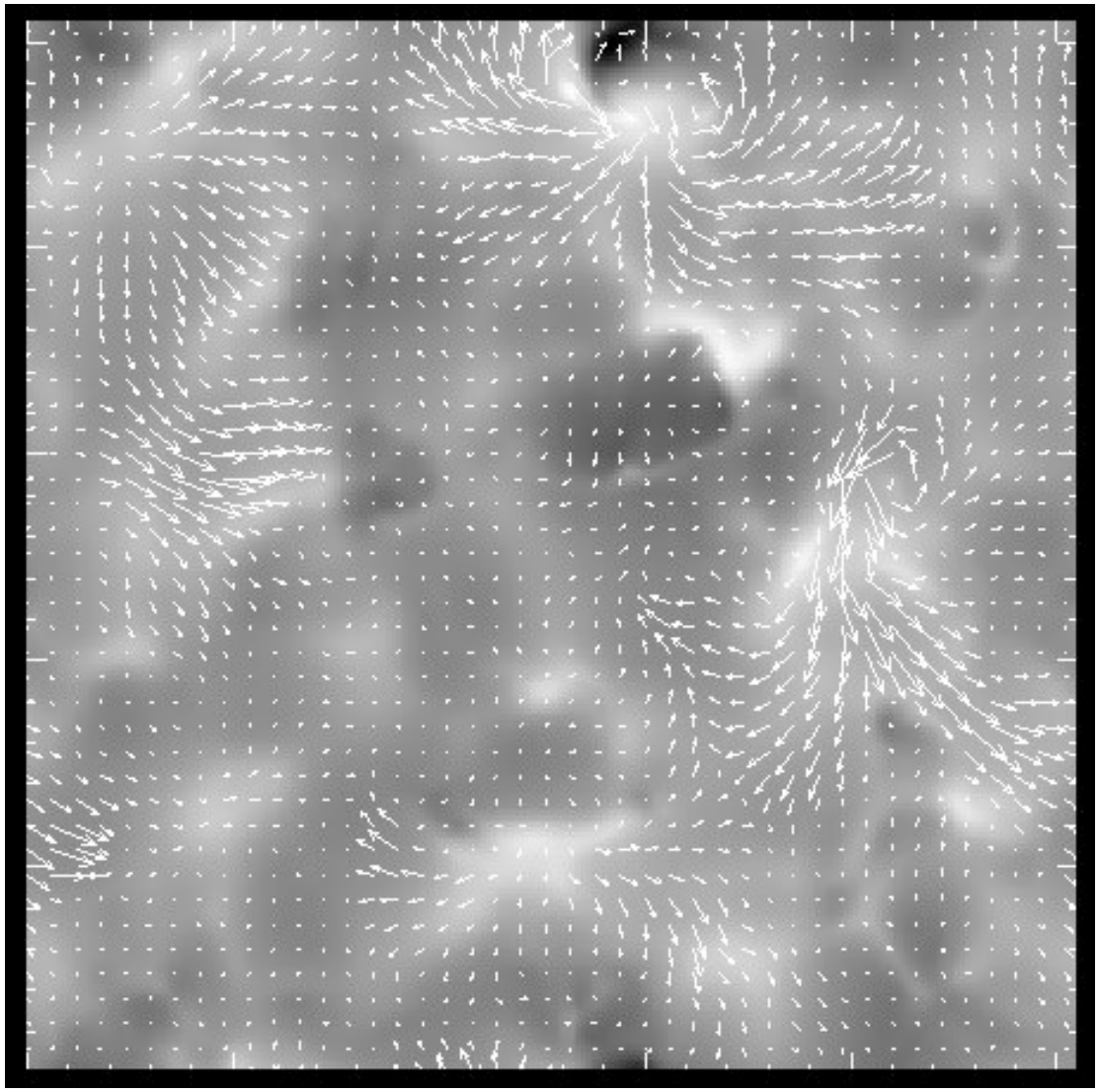

Vertical component of the magnetic field (grayscale) and the transverse flow pattern (vectors) in the model transition region.

A horizontal slice taken ~ 800 km above the model photosphere. Here the flows (and magnetic field) bear little resemblance to those seen at the photosphere.

An important question is whether similar disparities exist in active region complexes, and if so, what consequences does this have for estimates of magnetic energy and helicity before and after eruptive events?

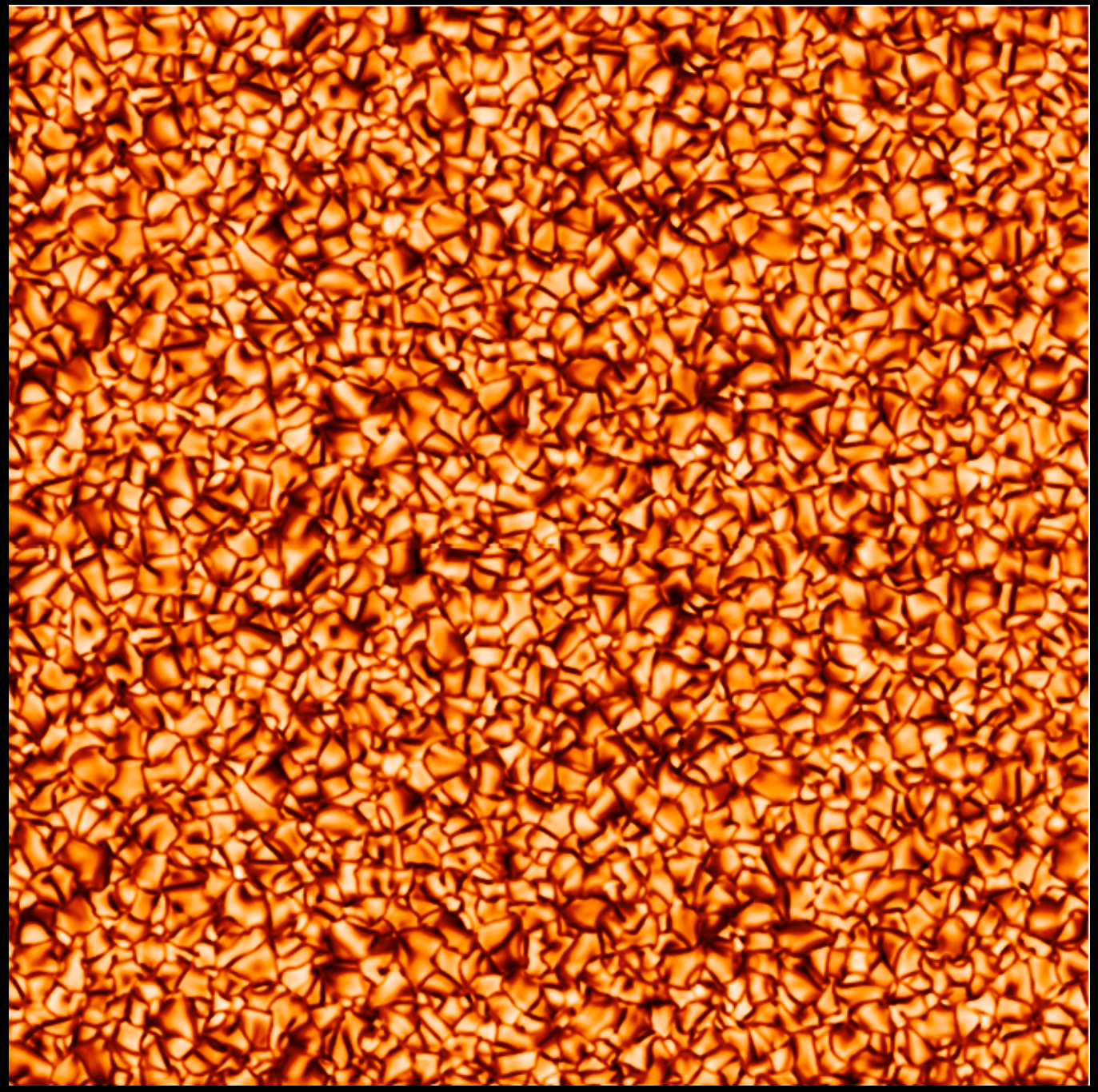

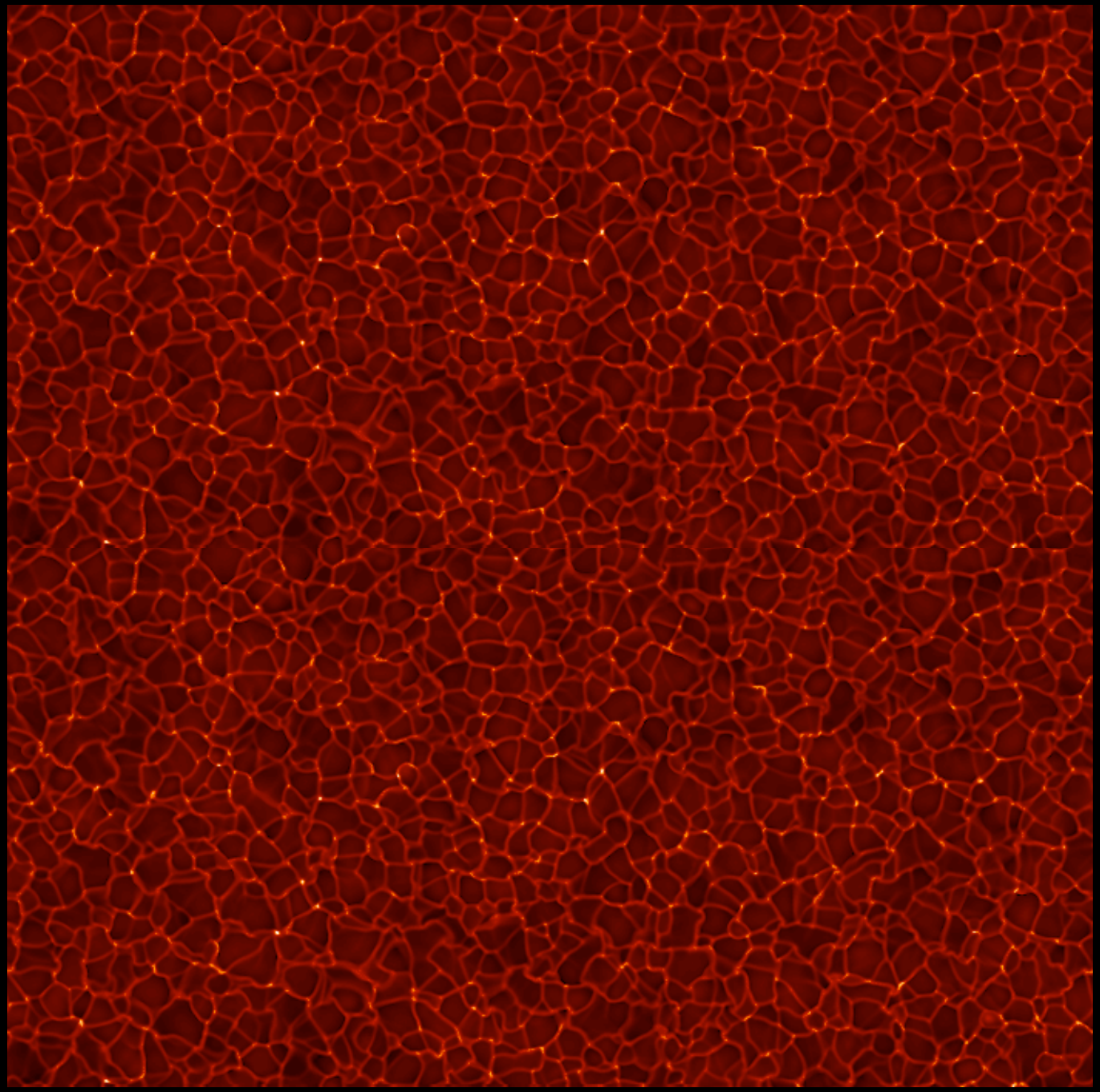

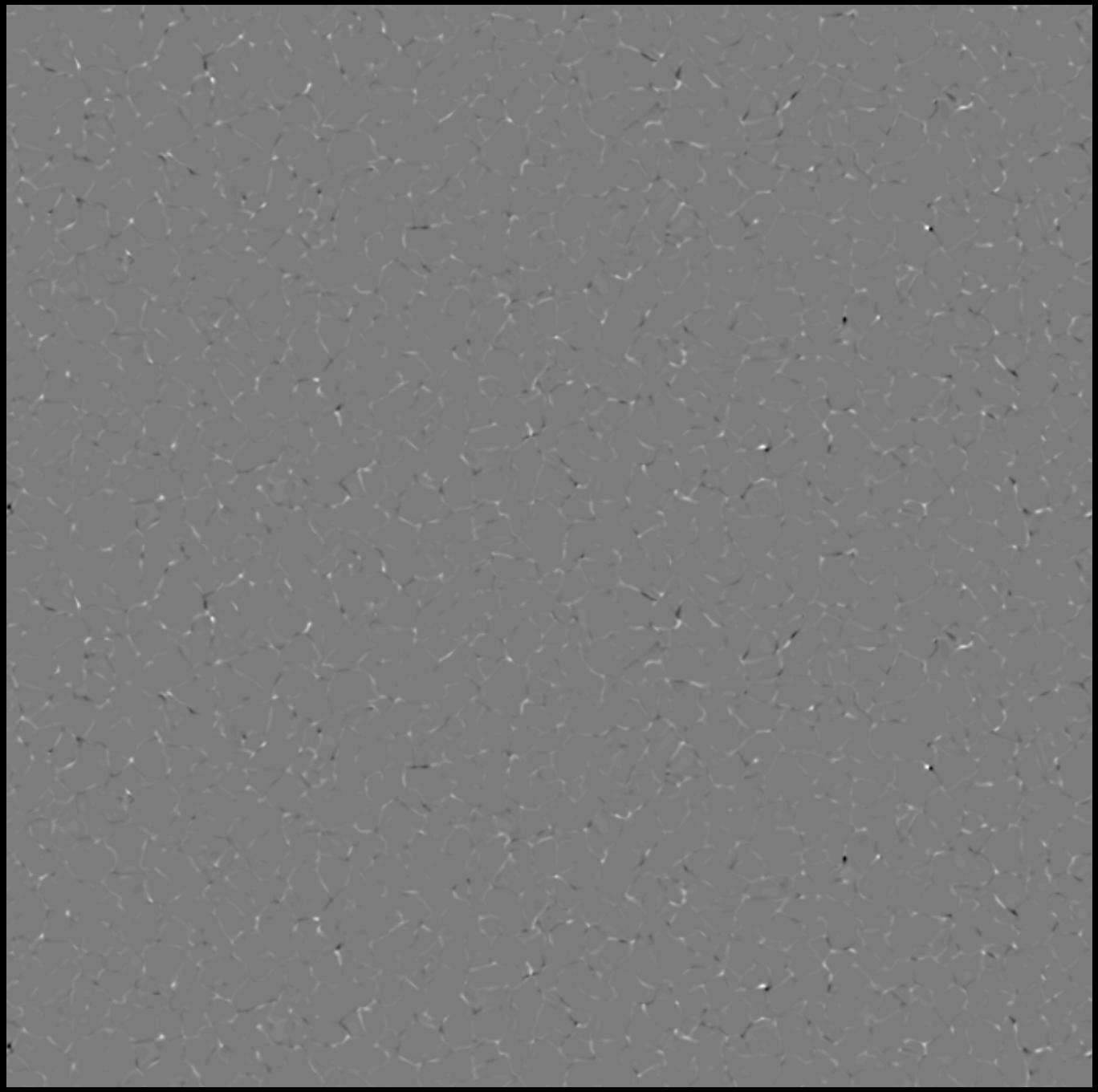

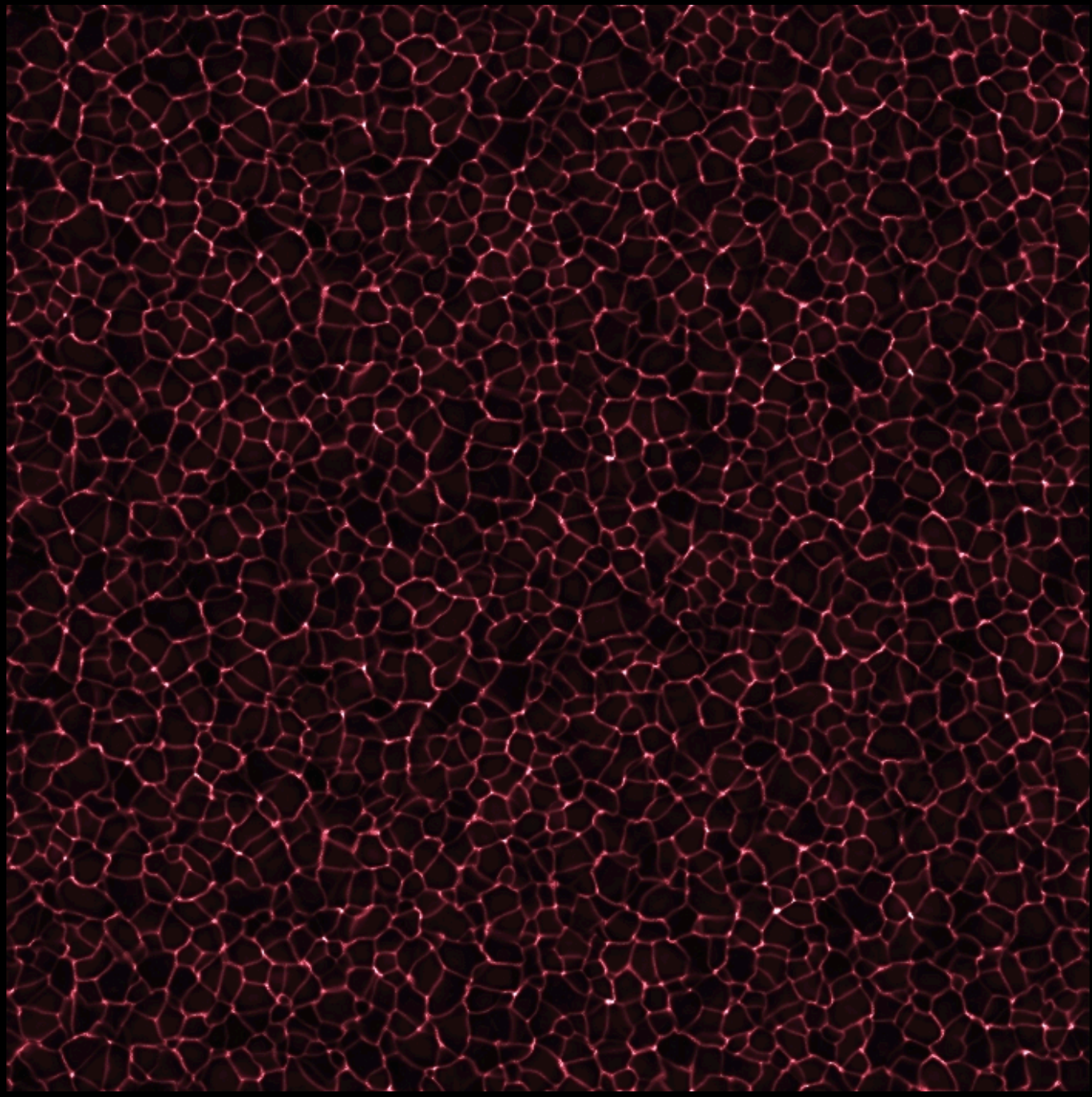

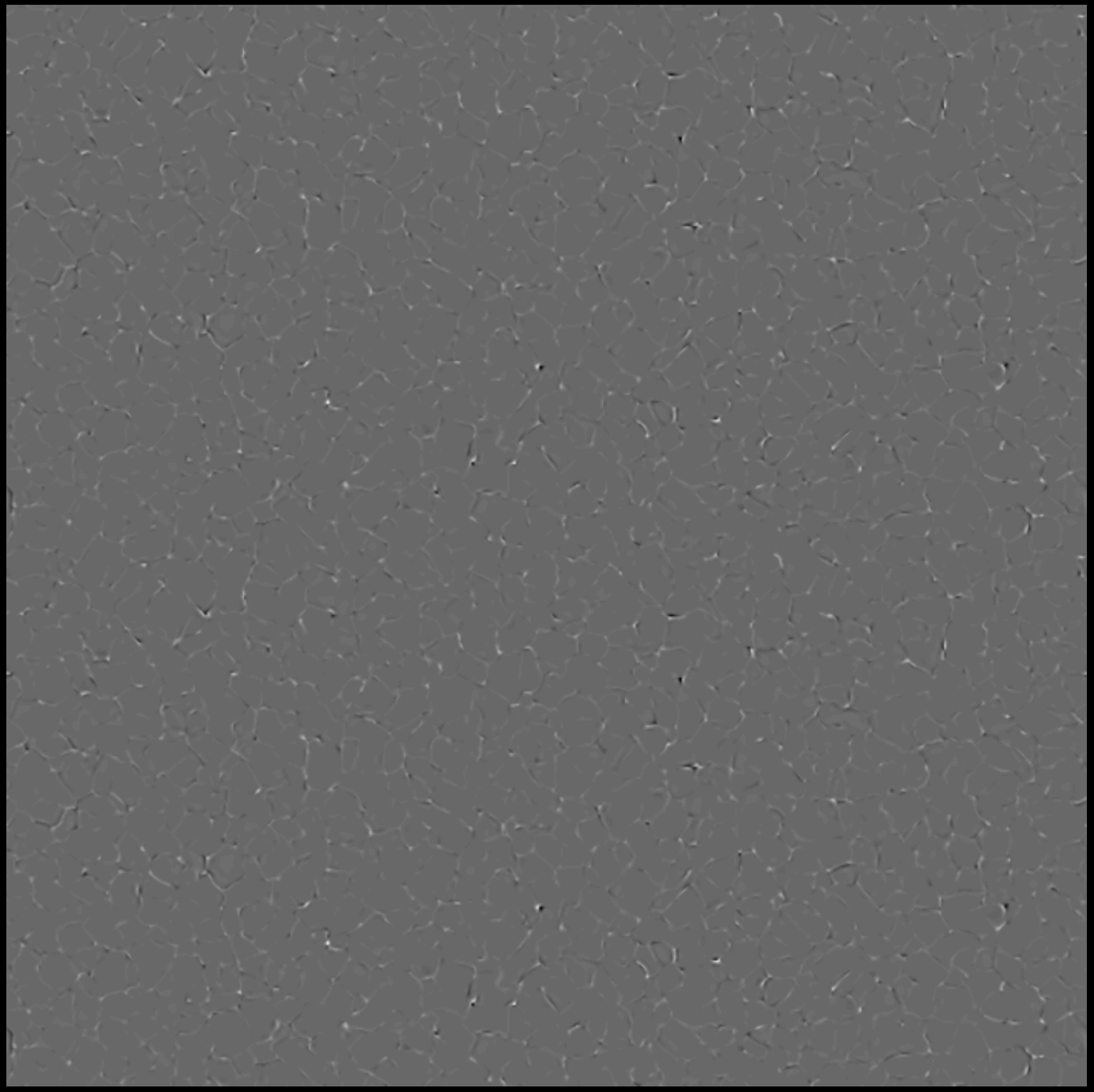

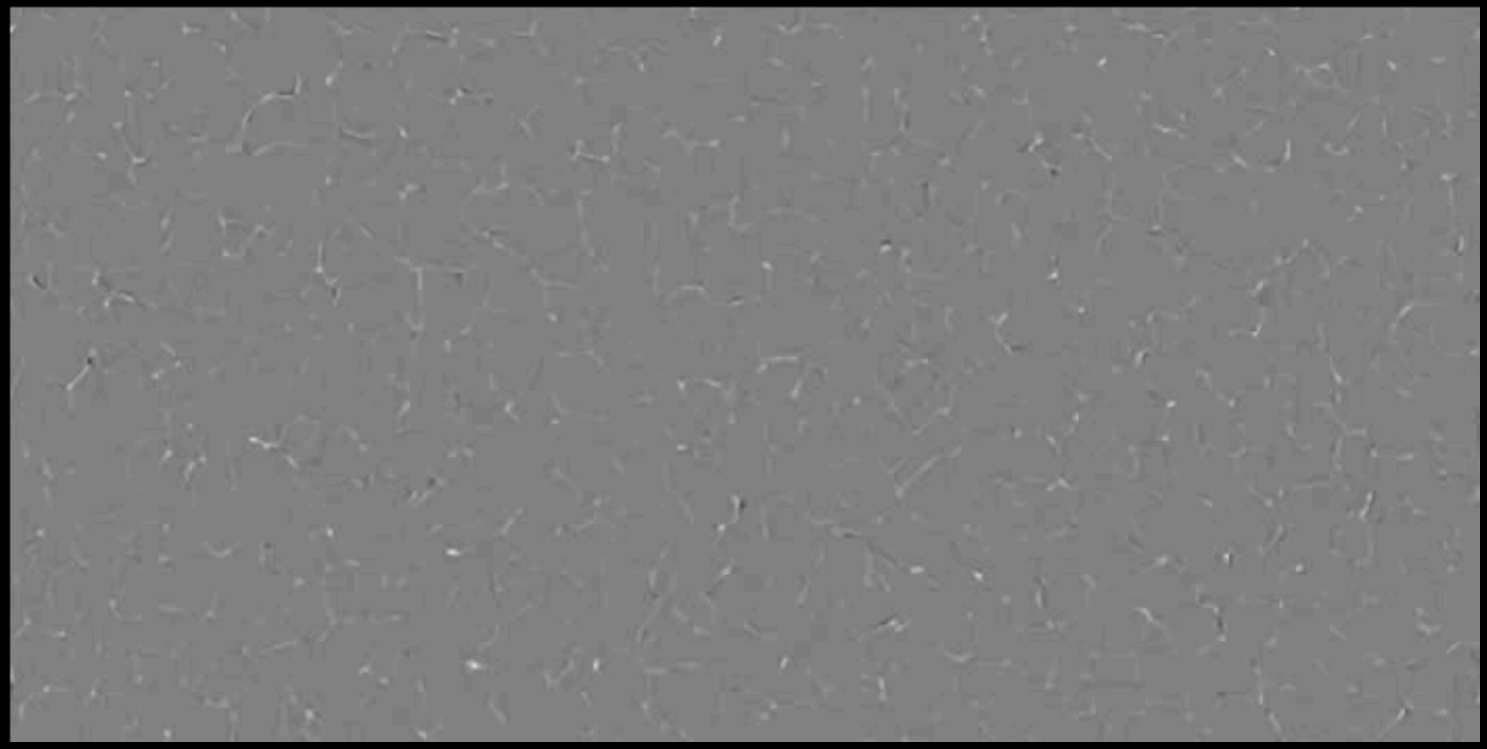

Vertical component of the magnetic field at the model photosphere

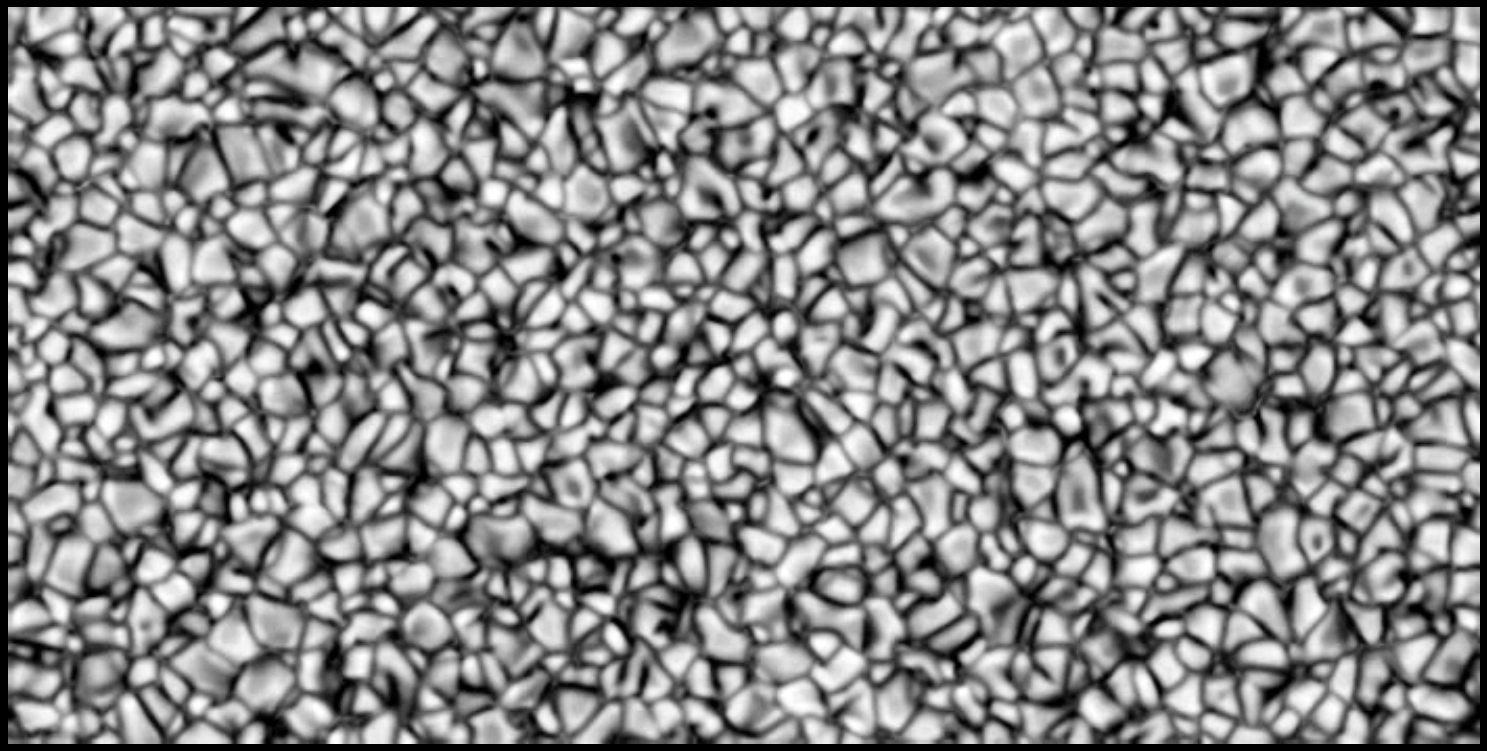

Gas temperature at the model photosphere

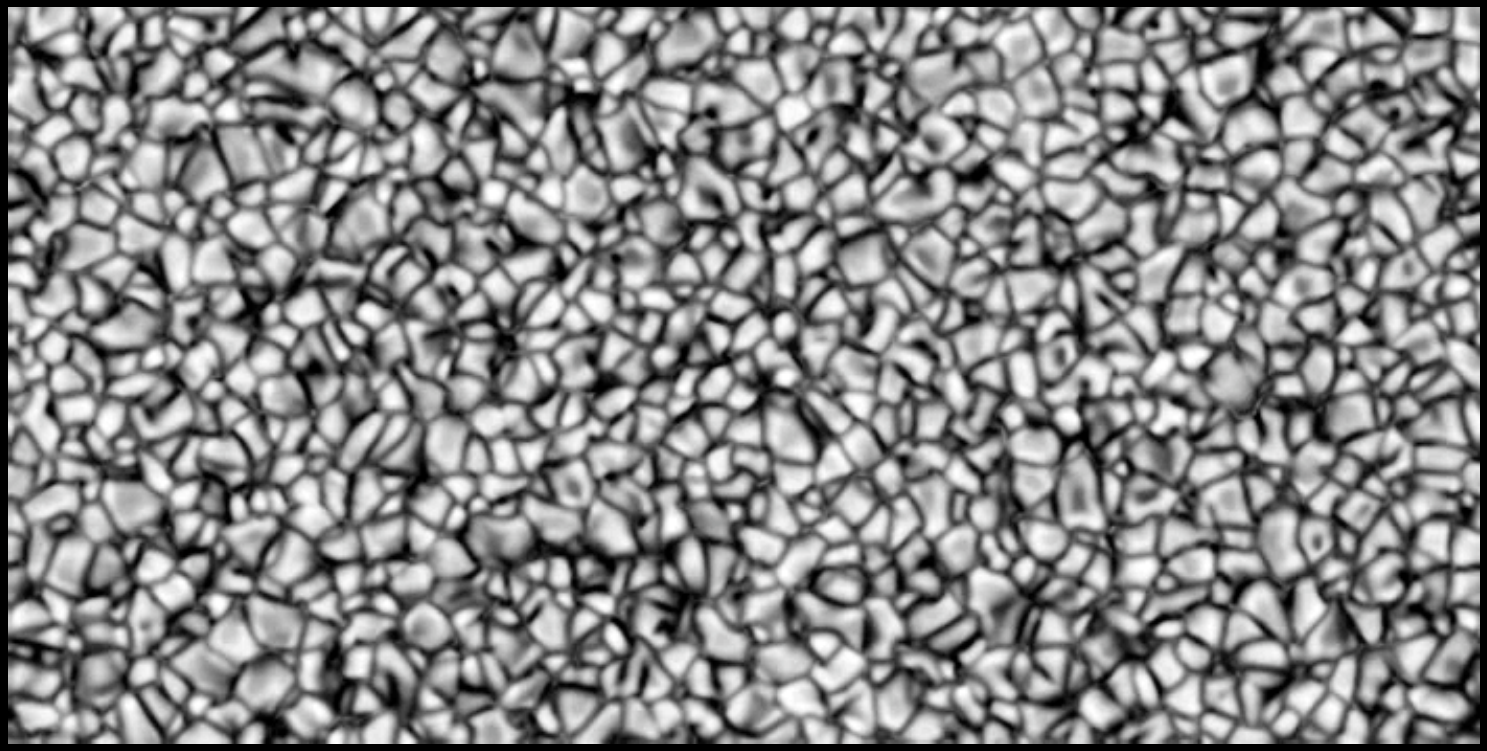

Gas temperature at the model photosphere (20 fps)

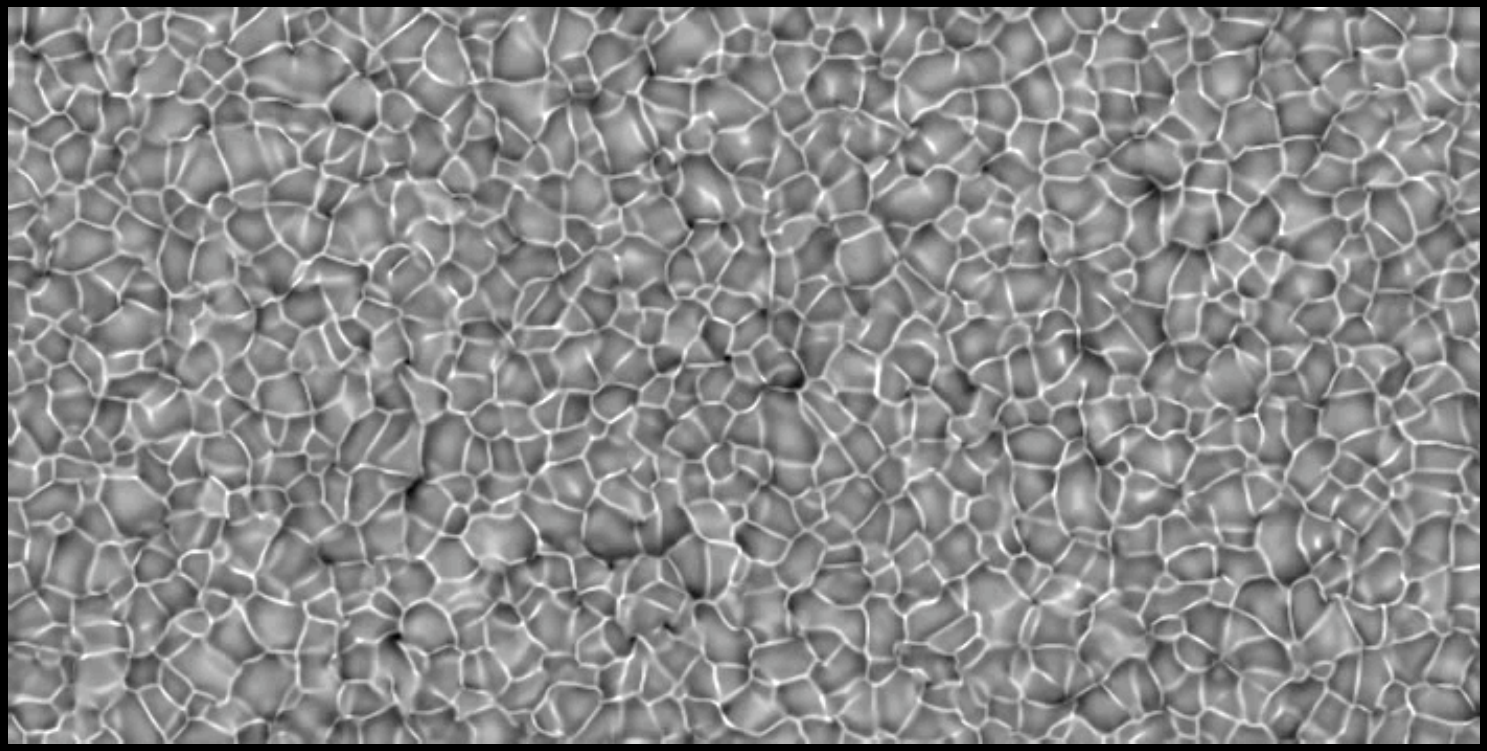

Gas density at the model photosphere

As an acid test of RADMHD's ability to dynamically evolve active region fields over realistic spatial scales, we initiate the following experiment:

- Thermally relax an active region-scale, field-free hydrodynamic model of surface convection.

- Adjust boundary conditions to accommodate the insertion of magnetic structures obtained from previous simulations of flux emergence in non-convective environments (see Abbett & Fisher 2003). This will allow us to study the interaction of emerged structures with granular flows as the system equilibrates, and will allow us to assess the efficiency of our current operator splitting scheme when relatively strong fields permeate the low density model corona.

- Adjust the empirical magnetic heating function (constrained only by an integral relationship) as necessary to achieve coronal temperatures and densities consistent with X-ray observations.

- Follow the magnetic connectivity of the active region as convective turbulence acts on loop footpoints, and the structure begins to decay.

Above: *The magnetic structure of the RADMHD model atmosphere*

Right: *The ANMHD sub-surface omega loop (Run SS3 from Abbett et al. 2000) used to emerge magnetic flux into the model atmosphere from below.*

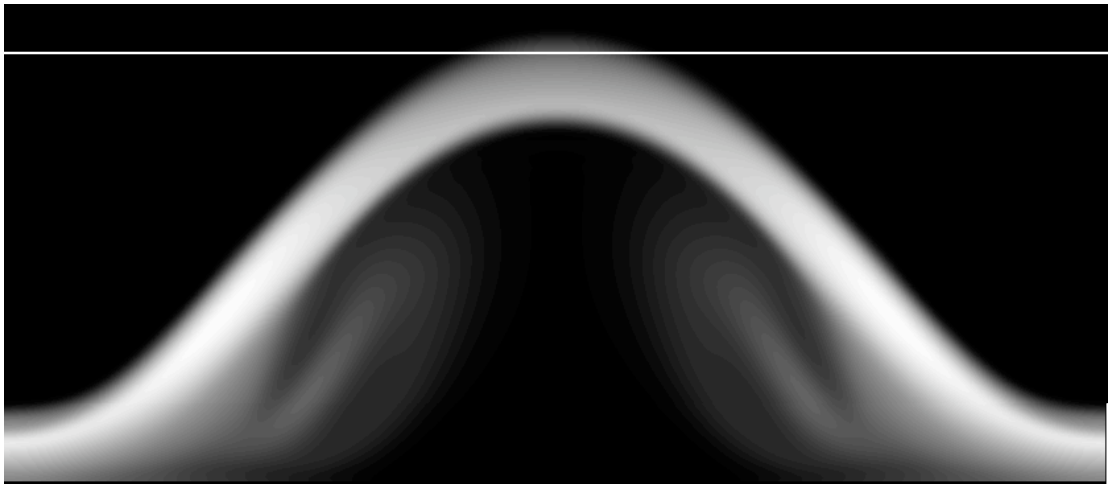

Coronal magnetic field above the newly emerged active region

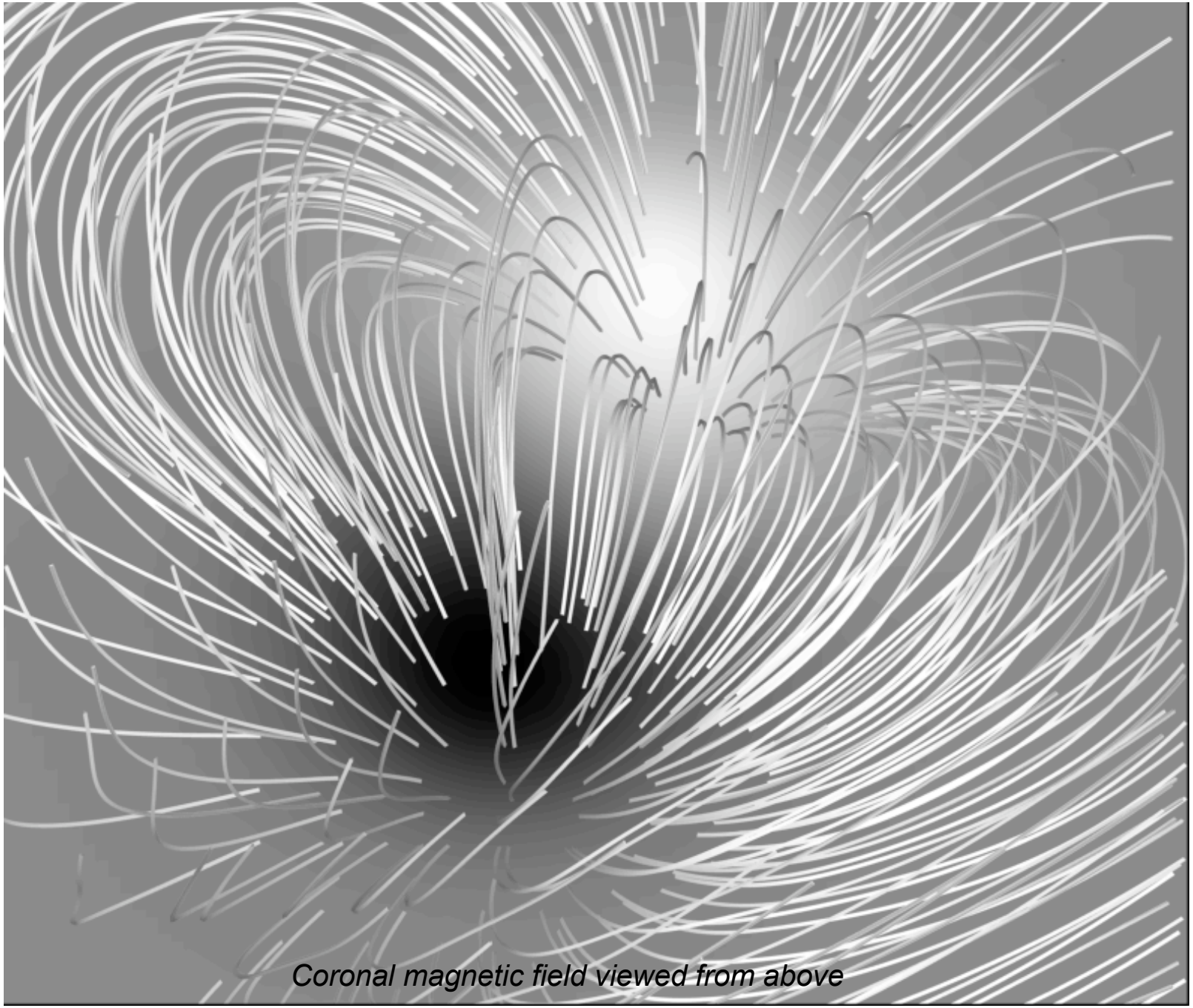

Coronal magnetic field viewed from above

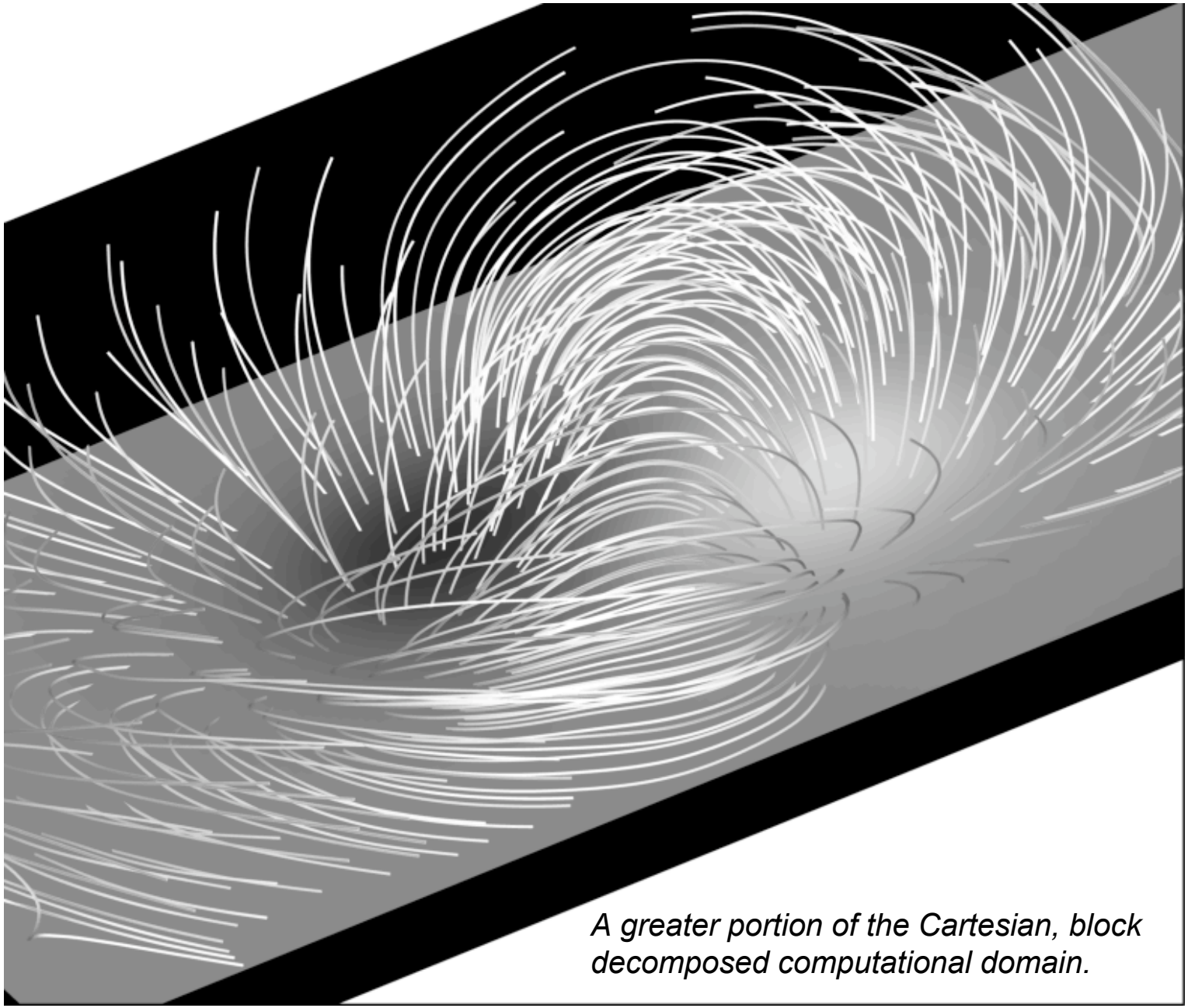

A greater portion of the Cartesian, block decomposed computational domain.

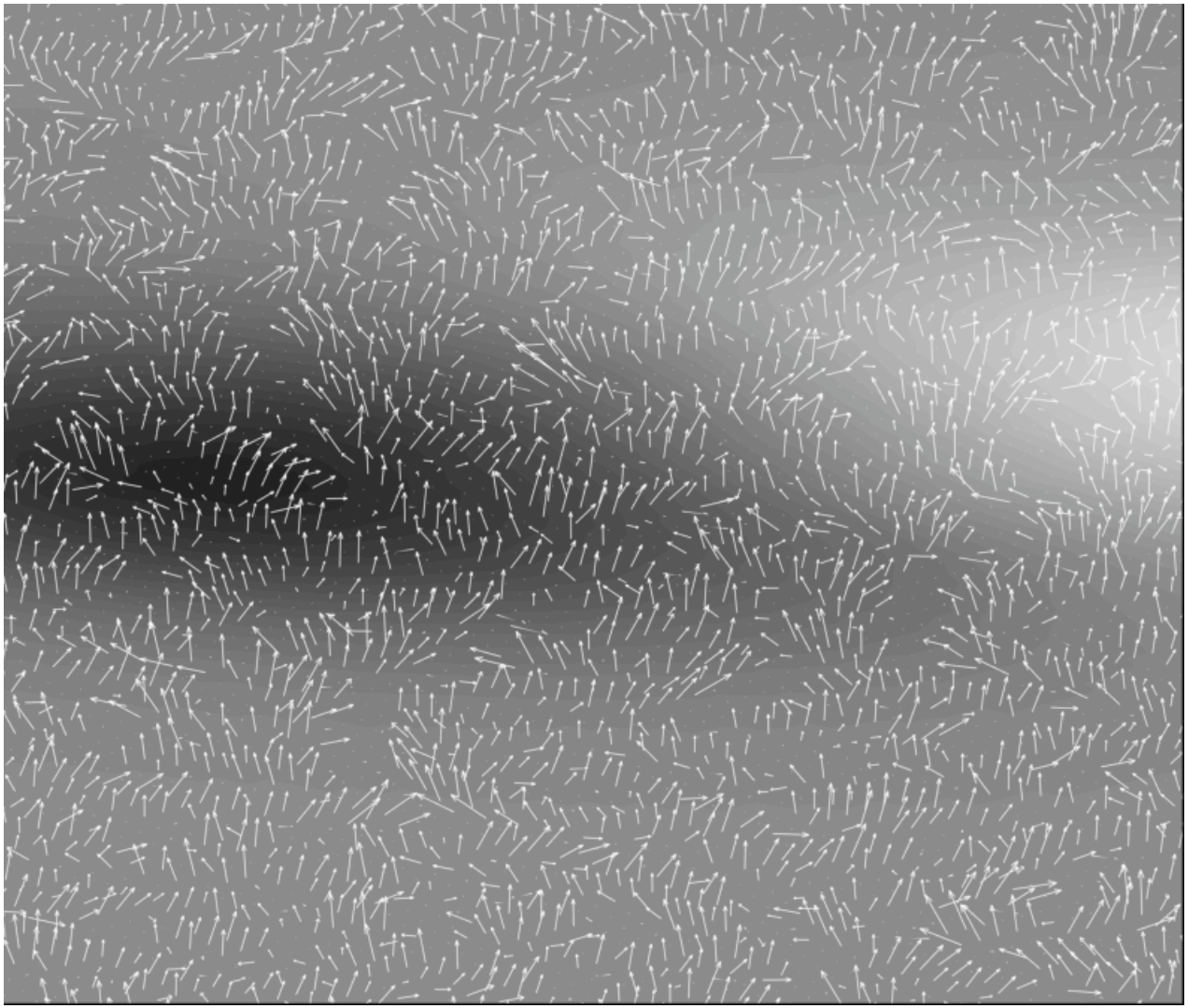

The small scale flow structure at the RADMHD model photosphere superimposed on a grayscale image of the vertical component of the magnetic field at the photosphere. Note that in this experiment, the large scale flows from ANMHD associated with the tube's emergence have not been included. This is an exploratory simulation of active region decay captured in its early stages.

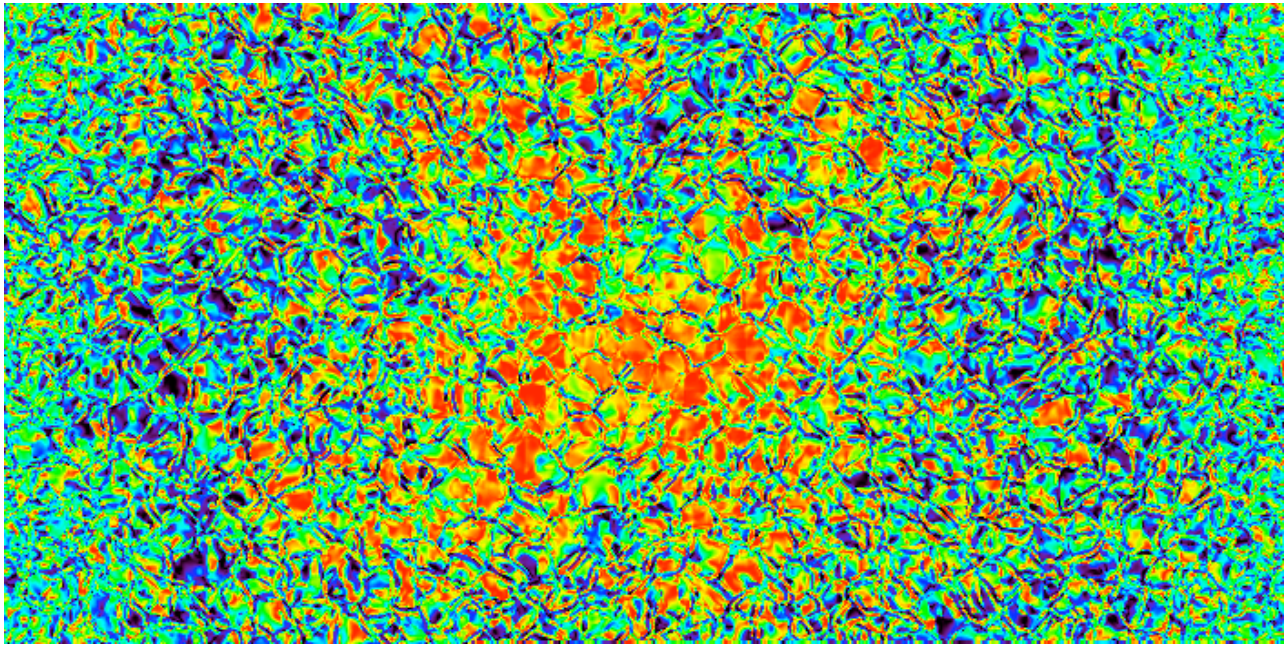

Model photosphere (above); model “chromosphere” (below)

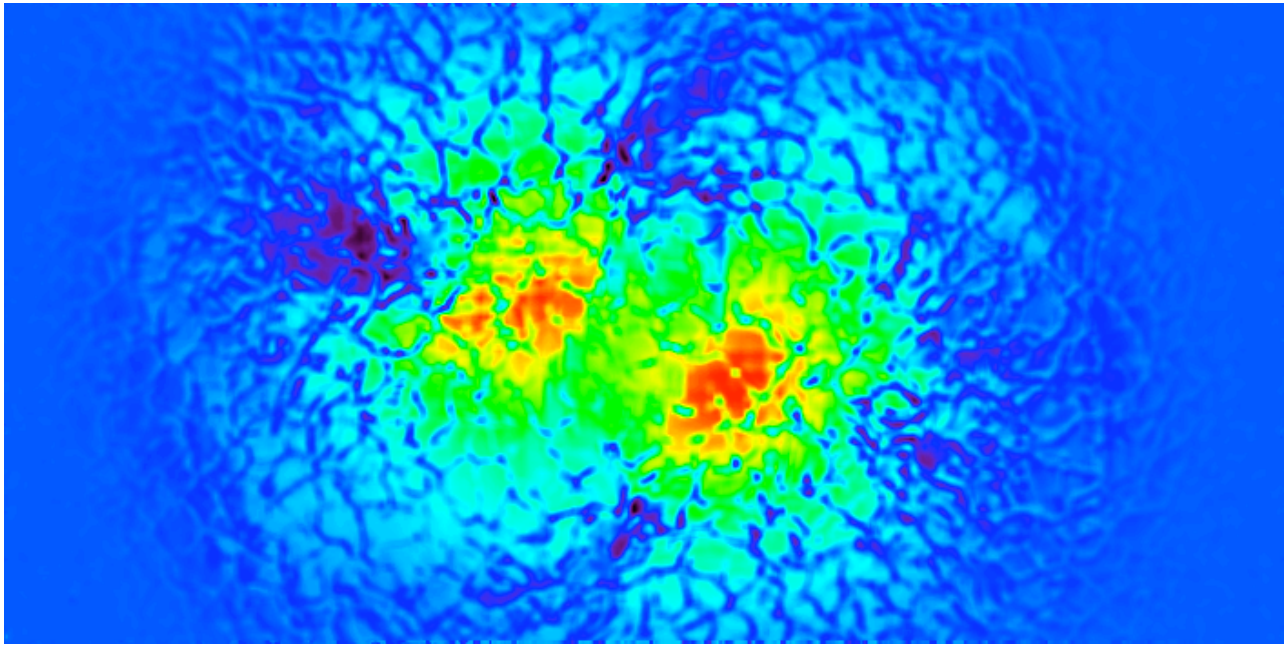

How force-free is the active region magnetic field in the low atmosphere?

Images on the left:

$$\alpha \equiv \frac{|\mathbf{J}\cdot\mathbf{B}|}{|\mathbf{J}||\mathbf{B}|}$$

Note: preliminary test calculations!

$$\alpha_B = \frac{\alpha\,|\mathbf{B}|}{\int |\mathbf{B}|\,dA}$$

Average field-weighted $\langle \alpha(z) \rangle = \dfrac{\int \alpha \, |\mathbf{B}| \, dA}{\int |\mathbf{B}| \, dA}$

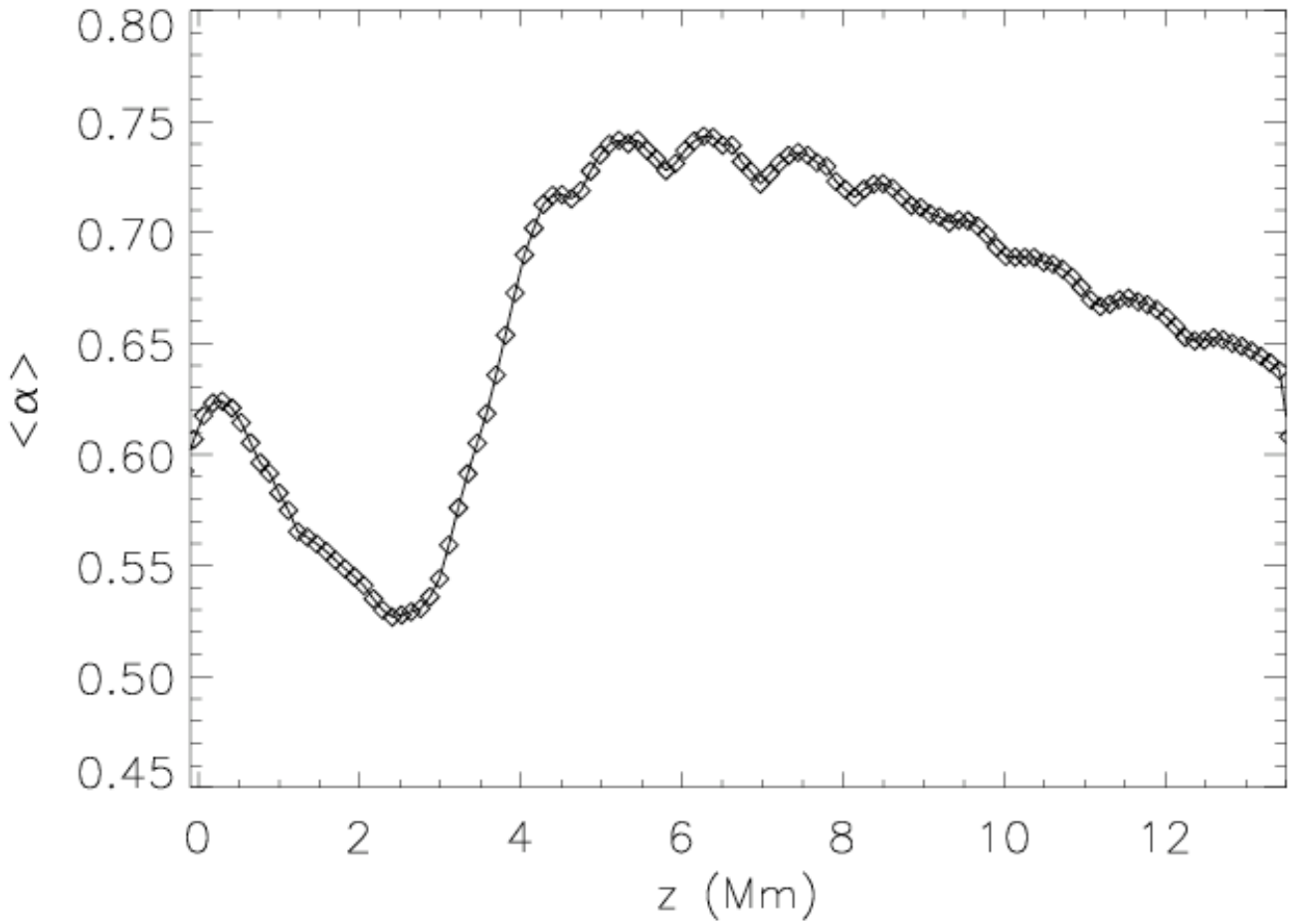

Summary:

We have begun a series of numerical simulations of active region magnetic fields over realistic spatial scales in a computational domain that includes the upper convection zone, photosphere, chromosphere, transition region, and low corona. We continue to make modifications to RADMHD's algorithms to more efficiently treat the spatial and temporal disparities of the combined system in the presence of strong active region fields. These exploratory simulations have been successful, and are ongoing. In the near future, we will report on more realistic simulations over a much larger spatial scale using a non-uniform mesh (i.e., the domain will be extended much farther out into the corona).

References:

Abbett, W. P., 2007, ApJ, **665**, 1469
Abbett, W.P., Fisher, G.H., Fan, Y., Bercik, D.J., 2004, ApJ **612**, 557
Bercik, D., 2002, Ph. D. thesis, Michigan State University
Bercik, D. J., Fisher, G. H., Johns-Krull, C. M., & Abbett, W. P., 2005, ApJ, **631**, 529
Knoll, D. A., & Keyes, D. E., 2003, J. Comp. Physics, **193**, 357
Kurganov, A., & Levy, D., 2000, SIAM J. Sci. Comput., **22**, 1461
Levy, D., Puppo, G., & Russo, G., 2000, SIAM J. Sci. Comput., **22**, 656
Lundquist, L. L., Fisher, G. H., McTiernan, J. M., & Leka, K. D., 2008 ApJ, in press.
Magara, T., 2004, ApJ, **605**, 480
Mikic, Z., Linker, J. A.,Titov, V., Lionello, R., & Riley, P., 2005, SHINE Workshop, July 11-15, Kona HI
Rogers, F. J., 2000, Physics of Plasmas, **7**, 51
Stein, R. F., Bercik, D., & Nordlund, A, 2003, ASP Conf. Ser. 286: Current Theoretical Models and Future High Resolution Solar Observations: Preparing for ATST, **286**, 121
Pevtsov, A. A., Fisher, G. H., Acton, L. W., Longcope, D. W., Johns-Krull, C. M., Kankelborg, C. C., & Metcalf, T. R. 2003, ApJ, **598**, 1387

Acknowledgments:

This work is funded in part by NASA's Heliophysics Theory and TR&T programs, and by the NSF's ATM program.